Chapter 83
Acquisition Time Performance of Initial Cell Search in 3GPP LTE System

You Zhou, Fei Qi and Hanying Hu

Abstract This paper focuses on shortening the mean time to acquire for initial cell search in the 3rd Generation Partnership Project (3GPP) Long Term Evolution (LTE) system. Exact result of mean time of the cell search is obtained by use of a state transition diagram of discrete-time Markov process for the acquisition process. From the deduced mean time formula, it can be seen that the false alarm probability plays a more important role in the acquisition time performance. In order to perform the initial cell search quickly, a new PSS detection structure which includes a verification module to suppress the false alarm is developed. Simulations show that the new structure can decrease the false alarm probability, and reduce the total acquisition time especially in the low SNR circumstance.

Keywords LTE · OFDM · Cell search · Acquisition time · Verification module

83.1 Introduction

3GPP LTE is recognized as the key technology for the next generation wireless communication system [1]. The LTE employs some advanced technologies which include Orthogonal Frequency Division Multiplexing (OFDM), Multiple Input Multiple Output (MIMO) and so on [1]. Demodulation of OFDM signal is vulnerable to timing offset and frequency offset. A User Equipment (UE) wishing to access an LTE cell must first undertake a cell search procedure, which is tightly connected to the Primary Synchronization Signal (PSS) and Secondary Synchronization Signal (SSS) transmitted by an LTE cell [2].

Y. Zhou (✉) · F. Qi · H. Hu
Zhengzhou Information Technology Institute, Zhengzhou, Henan, China
e-mail: emailzhouyou@sina.com

W. E. Wong and T. Ma (eds.), *Emerging Technologies for Information Systems, Computing, and Management*, Lecture Notes in Electrical Engineering 236, DOI: 10.1007/978-1-4614-7010-6_83,

The synchronization is a continuous and periodic process, which must be always active. So it is of significance to acquire it in a short time and the mean acquisition time of the cell search is a very important parameter to reflect the performance of the cell search structure. Currently, PSS detection in LTE has been studied considerably, and the topic lies in increasing the detection probability or simplifying the detection process. The classic maximum likelihood detector takes advantage of good autocorrelation and cross-correlation performance of PSS sequence in the time domain [3]. A normalized detection is proposed in order to avoid the confused detection of the peak sequence [4]. It firstly detects the cyclic prefix (CP) type which leads to the detection of symbol synchronization, and then acquires the PSS in the frequency domain which greatly simplifies the acquisition process [5]. It achieves a reliable PSS detection with a much lower complexity by exploiting the central-symmetric property of Zadoff-Chuf (ZC) sequences in the time domain [6].

In this paper we will focus on the mean acquisition time performance of initial cell search via a state transition diagram of discrete-time Markov process. From the numerical result of mean acquisition time, we find that false alarm property plays a more important role in the acquisition time performance. In order to perform the cell search quickly a new structure is developed to suppress the false alarm. The performance of the proposed structure is compared with that of normal PSS detection structure.

The remainder of this paper is organized as follows. A system model of PSS transmission and receiving is provided in Sect. 83.2. Section 83.3 deduces the mean time of the acquisition process and Sect. 83.4 introduces a new PSS detection structure. In Sect. 83.5, based on the numerology provided in the physical layer specification for 3G LTE, the performance of the proposed structure is investigated and compared with the normal detection structure. Finally the conclusions are drawn in Sect. 83.6.

83.2 System Signal Model

Let us firstly introduce the notation that will be adopted throughout the paper. Superscripts * denotes complex conjugate. $[\cdot]^T$ is the transpose of a matrix. $\mathrm{diag}\{\cdot\}$ is the diagonal matrix. A circularly symmetric complex Gaussian random variable w with mean m and variance σ^2 is denoted by $w \sim \mathcal{CN}(m, \sigma^2)$. The operator $|\cdot|$ returns the modulus of a complex number. $\mathrm{mod}(x, y)$ is the remainder operator. $\max(\mathbf{x})$ gives the maximum value of vector $\mathbf{x}$.

In LTE system, each cell is identified by the cell identification information carried by PSS and SSS. A length of 63 ZC sequence is used to generate the PSS, which occupies the central 72 sub-carriers [7], as illustrated in Fig. 83.1. It is transmitted every 5 ms.

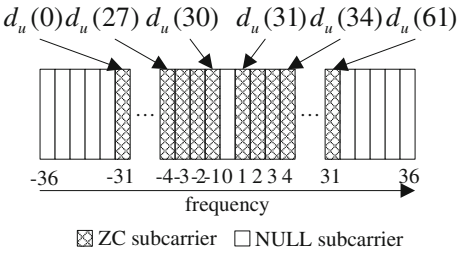

Fig. 83.1 PSS mapping of 3G LTE in the frequency domain

The sequence $d_u(n)$ is generated according to

$$d_u(n) = \begin{cases} \exp[-j\pi un(n+1)/63] & n = 0, 1, \ldots, 30 \\ \exp[-j\pi u(n+1)(n+2)/63] & n = 31, 32, \ldots, 61 \end{cases} \tag{83.1}$$

where the index u is depending on physical-layer identity $N_{ID}^{(2)}$ within the physical-layer cell-identity group. Without loss of generality, we use $\mathbf{x} = [0, d_u(31), \ldots, d_u(61), \mathbf{z}_1 \ldots \mathbf{z}_2, d_u(0), \ldots, d_u(30)]^T$ to represent the transmitted PSS vector, $\mathbf{z}_1$ and $\mathbf{z}_2$ are random transmitted symbols whose size depends on the bandwidth of the LTE system. The received PSS base-band signal on the antenna i is given by

$$\mathbf{r}_i = \mathbf{E}_i \mathbf{F} \mathbf{H}_i \mathbf{x} + \mathbf{w}_i \tag{83.2}$$

where $\mathbf{E}_i = \text{diag}\{1, e^{j2\pi\varepsilon_i/N_{fft}}, \ldots, e^{j2\pi\varepsilon_i(N_{fft}-1)/N_{fft}}\}$ with ε_i representing the normalized frequency offset (frequency offset normalized to a subcarrier spacing of OFDM symbols), N_{fft} is the FFT size, $\mathbf{F}$ is the IFFT matrix with $[\mathbf{F}]_{nk} = e^{\frac{j2\pi nk}{N_{fft}}}/\sqrt{N_{fft}}$, $\mathbf{H}_i = \text{diag}\{H_i(0), H_i(1), \ldots, H_i(N_{fft}-1)\}$ represents the frequency-domain channel attenuation matrix. $\mathbf{w}_i$ is a vector of additive white Gaussian noise with $\mathbf{w}_i[k] \sim \mathcal{CN}(0, \sigma_w^2)$. $\mathbf{y}_i$ will be fed to the PSS detection structure to perform the acquisition process.

83.3 Analysis of Mean Acquisition Time

There is no time limit for the acquisition process, since PSS is periodically transmitted. Therefore, it is almost certain that the whole system will be in an acquisition state and the measurement of performance lies in the mean acquisition time $\text{E}(T_{acq})$. We use a state transition diagram of discrete-time Markov process to describe the process of the initial acquisition in the LTE system, as shown in Fig. 83.2.

The points on the outer circle represent the false alarm state, and ones on the inner circle are detection points whose number depends on the PSS transmission period, synchronization window size and sampling frequency. Assuming that there are V possible detected points, and each is labeled from 1 to V. Among those

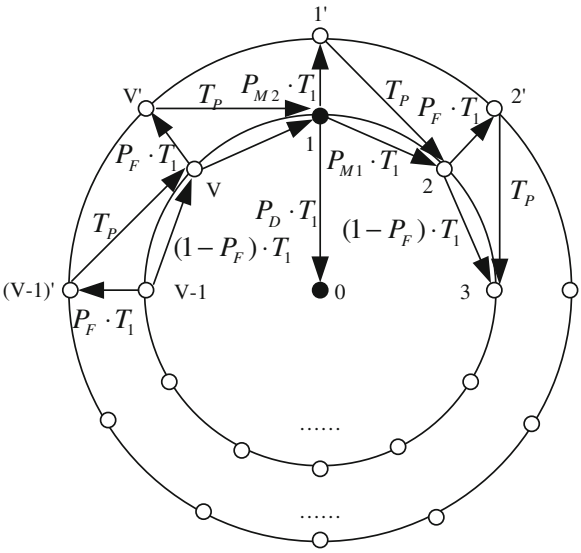

Fig. 83.2 Flow graph of 3G LTE initial cell search

points, there is only one point which corresponds to the collective state H_1 which is labeled as 1 with generalization, and the rest ones belong to false alarm state H_0. Each detected point corresponds to a false alarm state except for 1. Here a serial search strategy is adopted, any past time search information will not be used to change the search direction. The system will go to the next detected point after T_P seconds when a false alarm appears. The detection probability from 1 to 0 is P_D called detection probability. The missing probabilities from state 1 to $1'$ and 2 are P_{M2} and P_{M1}, which represents two kinds of missing scenarios, one is false detected PSS index, and the other is missing the timing point. The relationship is $P_{M1} + P_{M2} + P_D = 1$. The false alarm probability from i to i' $(i \neq 1)$ is P_F, and $1 - P_F$ indicates the probability from i to $i + 1$. Let z indicate the unit delay operator. Its value depends on the sampling rate. Furthermore, we can get the generating function from one point to the other,

$$H_{1\to 0}(z) = H_D(z) = P_D z \tag{83.3}$$

$$H_{i\to i+1}(z) = H_0(z) = (1 - P_F)z + P_F z^{K_p+1}, (i \neq 1) \tag{83.4}$$

$$H_{1\to 2}(z) = H_M(z) = P_{M1} z + P_{M2} z^{K_p+1} \tag{83.5}$$

Here we assume that $T_P = K_p T_1$. Then we can simplify Figs. 83.2–83.3. According to Mason formula [8], the generating function from i to 0 is

$$H_i(z) = \frac{H_D(z) H_0^{\mathrm{mod}(V-i+1,V)}(z)}{1 - H_M(z) H_0^{V-1}(z)} \tag{83.6}$$

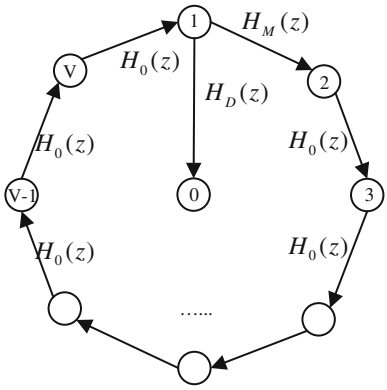

Fig. 83.3 Simplified flow graph of 3G LTE initial cell search

Since the search process can start at any one of the detection points, we assume that the probability follows uniform distribution with probability$1/V$. Then the generating function of the whole acquisition process follows that

$$\begin{aligned} H(z) &= \sum_{i=1}^{V} \frac{1}{V} H_i(z) = \frac{H_D(z)}{V\left[1 - H_M(z)H_0^{V-1}(z)\right]} \sum_{i=1}^{V} H_0^{\mathrm{mod}(V-i+1,V)}(z) \\ &= \frac{H_D(z)\left[1 - H_0^V(z)\right]}{V\left[1 - H_M(z)H_0^{V-1}(z)\right]\left[1 - H_0(z)\right]} \end{aligned} \tag{83.7}$$

The mean acquisition time can be expressed as [9, 10]

$$\begin{aligned} \bar{T}_{acq} &= \left.\frac{\partial H(z)}{\partial z}\right|_{z=1} \cdot T_1 \\ &= \frac{T_1}{H_D(1)}\left[H_D'(1) + H_M'(1) + (V-1)H_0'(1)\left[1 - \frac{H_D(1)}{2}\right]\right] \\ &\approx \frac{T_1}{P_D}\left[2 - P_D + (V-1)(K_P P_F + 1)(1 - \frac{P_D}{2})\right] \end{aligned} \tag{83.8}$$

Because of the PSS near perfect cross-correlation properties, it is reasonable to assume that $P_{M2} \ll 1$ during the derivation process.

Figure 83.4 shows $\bar{T}_{acq}$ trend with the change of different $P_D$and P_F according to Eq. (83.8), where $V = 1/153600$, $K_P = 307200$. $\bar{T}_{acq}$ decreases with the increase of P_D under certain P_F, while it increases with the increase of P_F under certain P_D. The relationship between $\bar{T}_{acq}$ and P_D, P_F is basically linear. $\bar{T}_{acq}$ equals to 2.5 ms with limited condition of $P_D = 1$ and $P_F = 0$. Furthermore, it is shown that P_F has a greater influence on $\bar{T}_{acq}$ than P_D, to which should be paid great attention.

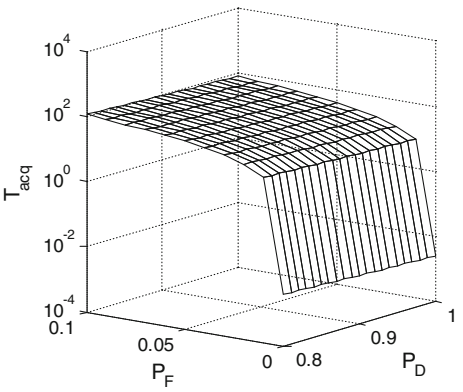

Fig. 83.4 Mean acquisition time with different P_F and P_D

83.4 PSS Detection Structure

From the previous discussion we can see that even a little increase of false alarm probability will lead to a great increase of mean acquisition time. Taking acquisition performance and complexity into account, we design a PSS acquisition structure shown in Fig. 83.5. At the first stage, it matches the received data from single antenna in the time domain to simplify the acquisition process. The sampled signal from one of the antennas is fed to a Low Pass Filter (LPF) with a pass bandwidth of 1.08 MHz. The maximum likelihood detector can be expressed as

$$(m, M) = \arg\max_{m,M} |\sum_{i=0}^{N-1} r'(i+m) S_M^*(i)|^2 \tag{83.9}$$

where $r'(i)$ represents the filtered signal, i is the time index, m is the timing offset, N is the FFT size, $S_M(i)$ is the local PSS replica with index M in the time domain. Having finished the first stage, received data from different antennas is performed with FFT. The corresponding PSS data is extracted to correlate with the local PSS replica in frequency domain which can be expressed as

$$A_u = \sum_{k=1}^{N_{ant}} |\sum_{i=0}^{61} R_k(i) d_{M'}^*(i)|^2 \tag{83.10}$$

where $R_k(i)$ is the received PSS data of antenna k in the frequency domain, N_{ant} is the number of antennas in the receiving system, and $d_{M'}(i)$ is local PSS replica with index M' in the frequency domain. During the second stage, the detector selects the index with the largest correlation value in the frequency domain.

$$M' = \arg\max_{M'} A_{M'} \tag{83.11}$$

If M' is identical with M, the whole PSS detection process is over, or go back to the first stage.

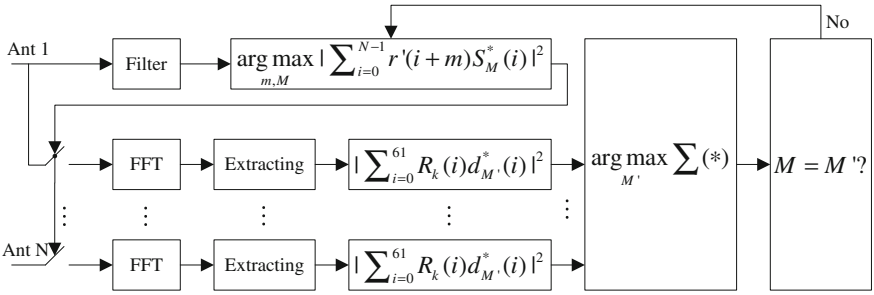

Fig. 83.5 PSS detection structure with verification module

The detection FFT module corresponding to each antenna can be multiplexed with FFT module used for OFDM demodulation. Also there are only 62 subcarriers containing PSS, so the increase of computation of the proposed structure is very small.

83.5 Simulations

Simulation parameters are based on the numerology in the 3G LTE physical layer specification [7]. Maximum frequency offset is 2 kHz and extended typical urban channel model (ETU) is used [11].

Figure 83.6 shows the false alarm performance comparison between normal structure (NS) and proposed structure (PS) with different number of antennas. Normal structure is detection structure without the verification module in the frequency domain. From the figure, we can see that PS has a better performance than that of NS, while PS with 4 antennas is better than PS with 2 antennas, especially for low SNR. The difference is becoming smaller and smaller along

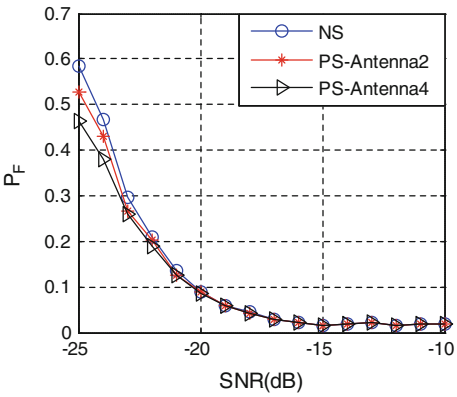

Fig. 83.6 P_F comparison between the two structures

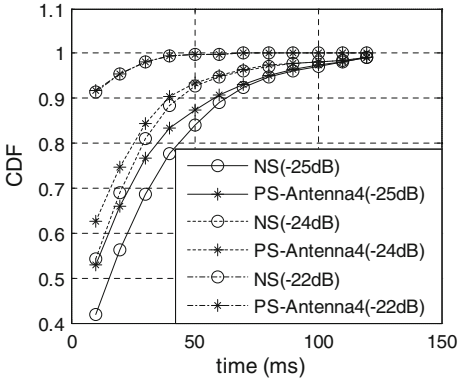

Fig. 83.7 CDF of cell search time comparison between the two structures

with the increase of SNR. The reason is that large SNR means a high credibility of the first stage, under which scenario the effect of verification module is weakened.

Figure 83.7 shows the CDF of cell search time of the two structures. It can be seen that the CDF of both structures is increasing along with the time while PS has a better performance than that of NS. Scenarios with different SNR have different kinds of performance. Lower SNR means larger difference in CDF performance between the two structures. The superiority of PS over NS is weakened with the increase of SNR. Cell search time also have an impact on the CDF performance. The advantage of PS finally disappears over the time.

83.6 Conclusion

In this paper, the mean time of initial cell search in 3GPP LTE system is studied, from which it can be found that the false alarm probability plays a more important role in the acquisition time performance. A novel PSS detection structure is proposed to suppress the false alarm by adding a verification module. Simulation results show that the proposed structure can decrease the false alarm probability, and reduce the total acquisition time especially in the low SNR circumstance.

References

1. Zhang, X., Tian, T., Zhou, X., Wen, Z.: LTE air interface technology and performance, pp. 1–6. Posts & Telecom press, Beijing (2009)
2. Shen, J., Suo, S., Quan, H., Zhao, X., Hu, H., Jiang, Y.: 3GPP long term evolution: principle and system design, pp. 280–300. Posts & Telecom press, Beijing (2009)
3. Sesia, S., Toufik, I., Baker, M.: LTE—the UMTS long term evolution, from theory to practice, pp.148–150. Wiley, New York (2009)

4. Silva, E.M., Dolecek, G.J., Harris, F.J.: Cell search in long term evolution systems: Primary and secondary synchronization. In: IEEE Third Latin American Symposium on Circuits and Systems, pp. 1–4 (2012)
5. Kim, Y.B., Chang, K.H.: Complexity optimized CP length pre-decision metric for cell searcher in the downlink of 3GPP LTE system. In: IEEE 20th International Symposium on Personal, Indoor and Mobile Radio Communications, pp.895–899 (2009)
6. Zhang, Z., Liu, J., Long, K.: Low-complexity cell search with fast PSS identification in LTE. IEEE Trans. Veh. Technol. **61**(4), 1719–1729 (2012)
7. 3GPP TS 36.211 v10.4.0, Technical specification group radio access network: Evolved universal terrestrial radio access, physical channels and modulation (Release 10) (2011)
8. Wu, D., Yang, L., Zhang, Y.: Signal and linear system analysis, pp. 350–357. Higher Education Press, Beijing (2006)
9. Polydoros, A., Weber, C.L.: A unified approach to serial search spread-spectrum code acquisition-part I: General theory. IEEE Trans. Commun. **32**(5), 542–549 (1984)
10. Polydoros, A., Weber, C.L.: A unified approach to serial search spread-spectrum code acquisition-part II: A matched-filter receiver. IEEE Trans. Commun. **32**(5), 550–560 (1984)
11. 3GPP TS 36.101 v10.6.0, Technical specification group radio access network: Evolved universal terrestrial radio access, user equipment radio transmission and reception (Release 10) (2012)